Lewis Base Catalyzed, Enantioselective Aldol Addition of Methyl Trichlorosilyl Ketene Acetal to Ketones

3 AUTHORS, INCLUDING:

Yu Fan

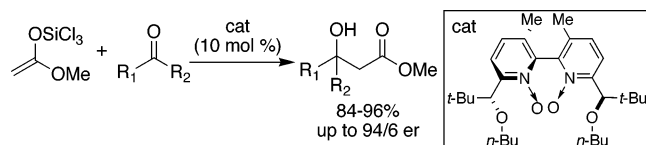Bristol-Myers Squibb

6 PUBLICATIONS   **475** CITATIONS

Lewis Base Catalyzed, Enantioselective Aldol Addition of Methyl Trichlorosilyl Ketene Acetal to Ketones

Scott E. Denmark,* Yu Fan, and Martin D. Eastgate

Roger Adams Laboratory, Department of Chemistry, University of Illinois, Urbana, Illinois 61801

denmark@scs.uiuc.edu

The catalytic enantioselective addition of an acetate enolate equivalent to ketones is described. Methyl trichlorosilyl ketene acetal reacts with a wide range of ketones in the presence of pyridine *N*-oxide to afford the aldol addition products in excellent yields. Chiral 2,2′-pyridyl bis-*N*-oxides bearing various substituents at the 3,3′- and 6,6′-positions also provide excellent yields of the aldol products with variable enantioselectivities ranging from 94/6 er for aromatic ketones to nearly racemic for aliphatic ketones. An X-ray crystal structure of the complex between a catalyst and silicon tetrachloride (((*P*)-(*R*,*R*)-**19**·SiCl₄)) has been obtained. Extensive computational analysis provides a stereochemical rationale for the observed trends in enantioselectivities.

Introduction

Stereocontrolled aldol additions to ketone acceptors provide direct access to chiral tertiary alcohols, ubiquitous subunits present in biologically active natural products.[1] However, despite the obvious synthetic potential of such a method, a general catalytic, enantioselective variant of the aldol addition reaction with ketones is still lacking. In light of recent advances in the development of catalytic, asymmetric aldol additions to aldehydes,[2] the absence of analogous methods for ketone acceptors is noteworthy but not surprising. Two critical challenges are readily apparent: the intrinsic endothermicity of the aldol additions to ketones[3] and the ability of a chiral catalyst to discriminate between the enantiotopic faces of a carbonyl group[4] flanked by two substituents with similar steric and electronic properties.[5,6]

There is only one example of a catalytic, enantioselective aldol addition to ketone acceptors, but this involves the use of highly activated α-ketoesters and α-diketones. Evans and co-workers have described catalytic, enantioselective additions of trialkylsilyl thioketene acetals to these activated α-dicarbonyl acceptors.[7] However, for nonactivated ketone acceptors,[8] the use of chiral auxiliaries attached to either reaction partner are needed to

(1) Selected examples: (a) Spongistatin 1: Pettit, G. R.; Chicacz, Z. A.; Gao, F,; Herald, C. L.; Boyd, M. R.; Schmidt, J. M.; Hooper, J. N. A. *J. Org. Chem*. **1993**, *58*, 1302−1304. (b) Camptothecin: Wall, M. E.; Wani, M. C.; Cook, C. E.; Palmer, K. H.; McPhail, A. T.; Sim, G. A. *J. Am. Chem. Soc*. **1966**, *88*, 3888−3890. (c) Amphidinolide B: Ishibashi, M.; Ohizumi, Y.; Hamashima, M.; Nakamura, H.; Hirata, Y.; Sasaki, T.; Kobayashi, J. *J. Chem. Soc., Chem. Commun*. **1987**, 1127−1129. (d) Apoptolidin: Hayakawa, Y.; Kim, J. W.; Adachi, H.; Shinya, K.; Fujita, K.-i.; Seto, H. *J. Am. Chem. Soc*. **1998**, *120*, 3524−3525. (e) Fostriecin: Tunac, J. B.; Graham, B. D.; Dobson, W. E. *J. Antibiot*. **1983**, *36*, 1595−1600.

(2) For recent authoritative reviews, see: (a) Nelson, S. G. *Tetrahedron: Asymmetry* **1998**, *9,* 357−389. (b) Carreira, E. M. In *Comprehensive Asymmetric Catalysis;* Jacobsen, E. N., Pfaltz, A., Yamamoto, H., Eds.; Springer-Verlag: Heidelberg, 1999; Vol. III, Chapter 29.1. (c) Carreira, E. M. In *Modern Carbonyl Chemistry*; Otera, J., Ed.; Wiley-VCH: Weinheim, 2000; Chapter 8. (d) Carreira, E. M. In *Catalytic Asymmetric Synthesis*, 2nd ed.; Ojima, I., Ed.; Wiley-VCH: Weinheim, 2000; Chapter 8B2. (e) *Modern Aldol Reactions*; Mahrwald, R., Ed.; Wiley-VCH: Weinheim, 2004.

(3) For a discussion of this problem in general, see: (a) Heathcock, C. H. In *Comprehensive Organic Synthesis: Additions to C−X π-Bonds Part 2*; Heathcock, C. H., Ed. Pergamon Press: Oxford, 1991; Chapter 1.5.

(4) Saito, S.; Yamamoto, H. In *Modern Carbonyl Reactions*; Otera, J., Ed.; Wiley-VCH: Weinheim, 2000; Chapter 2.

(5) For catalytic enantioselective organometallic additions to ketones, see: (a) Dosa, P. I.; Fu, G. C. *J. Am. Chem. Soc*. **1998**, *120*, 445−446. (b) Ramón, D. J.; Yus, M. *Tetrahedron* **1998**, *54*, 5651−5666. (c) Casolari, S.; D'Addario, D.; Tagliavini, E. *Org. Lett*. **1999**, *1*, 1061−63. (d) Weber, B.; Seebach, D. *Angew. Chem., Int. Ed*. **1992**, *31*, 84−85. (e) Garcia, C.; LaRochelle, L. K.; Walsh, P. J. *J. Am. Chem. Soc*. **2002**, *124*, 10970−10971. (f) Jeon, S.-J.; Walsh, P. J. *J. Am. Chem. Soc*. **2003**, *125*, 9544−9545. (g) DiMauro, E. F.; Kozlowski, M. C. *J. Am. Chem. Soc*. **2002**, *124*, 12668−12669.

(6) For catalytic enantioselective cyanosilylations of ketones, see: (a) Hamashima, Y.; Kanai, M.; Shibasaki, M. *J. Am. Chem. Soc*. **2000**, *122*, 7412−7413. (b) Yabu, K.; Masumoto, S.; Yamasaki, S.; Hamashima, Y.; Kanai, M.; Du, W.; Curran, D. P.; Shibasaki, M. *J. Am. Chem. Soc*. **2001**, *123*, 9908−9909. (c) Hamashima, Y.; Kanai, M.; Shibasaki, M. *Tetrahedron Lett*. **2001**, *42*, 691−694. (d) Tian, S.-K.; Deng, L. *J. Am. Chem. Soc*. **2001**, *123*, 6195−6196. (e) Tian, S.-K.; Hong, R.; Deng, L. *J. Am. Chem. Soc*. **2003**, *125*, 9900−9901.
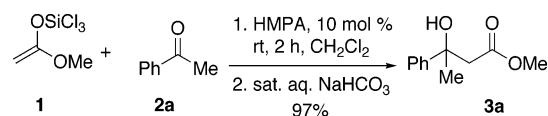
control the stereochemical outcome.[9,10] High diastereo-selectivities have been obtained in the additions of achiral enolates to chiral ketones bearing an α-sulfinyl[9a] or carbohydrate auxiliary.[10d] Significant progress has also been made in the development of various chiral enolates for the aldol addition to ketones. Excellent diastereoselectivities are observed in the additions of in-situ generated, chiral, titanium or zinc enolates to achiral ketones.[10b−e] Recently, the use of chiral amino alcohol additives has reported for stereocontrol in Reformatsky-type reactions.[11] Through large-scale screening, Ojida and co-workers discovered that cinchonin is highly effective in controlling the stereochemical outcome of Reformatsky-type reactions with heteroaromatic ketones.[11c]

Background

In recent years, we have been engaged in the development of catalytic asymmetric aldol addition reactions through application of *Lewis base catalysis*. In these reactions, chiral Lewis base activators promote the addition of enoxytrichlorosilane reagents derived from aldehydes, ketones, and esters to a wide variety of aldehydes with high diastereo- and enantioselectivity. Although ketone- and aldehyde-derived enoxytrichlorosilanes do not react with ketones, the trichlorosilyl ketene acetal of methyl acetate **1** was shown to be sufficiently reactive in early studies of this aldol process.[12] Silyl ketene acetal **1** reacts slowly with acetophenone **2a** at room temperature, but in the presence of a catalytic amount of HMPA, a rapid addition takes place affording a high yield of aldol product **3a** (Scheme 1). This preliminaryresult showed that additions of **1** to ketones were thermodynamically favorable and also susceptible to Lewis base catalysis.

We therefore embarked on a program to develop a general catalytic, enantioselective method for aldol additions to ketones with **1**. The primary goals of this study

(7) (a) Evans, D. A.; Burgey, C. S.; Kozlowski, M. C.; Tregay, S. W. *J. Am. Chem. Soc.* **1999**, *121*, 686−699. (b) Evans, D. A.; Kozlowski, M. C.; Burgey, C. S.; MacMillan, D. W. C. *J. Am. Chem. Soc.* **1997**, *119*, 7893−7894.

(8) Shibasaki has recently described a catalytic aldol addition of trialkylsilyl ketene acetals to ketones. One example of an enantioselective addition to 3-pentanone was reported. Oisaki, K.; Suto, Y.; Kanai, M.; Shibasaki, M. *J. Am. Chem. Soc.* **2003**, *125*, 5644−5.

(9) For additions of achiral enolates to ketones with chiral auxiliaries, see: (a) Ruano, J. L. G.; Barros, D.; Carmen Maestro, M.; Slawin, A. M. Z.; Bulman, P. C. *J. Org. Chem.* **2000**, *65*, 6027−6034. (b) Mioskowski, C.; Solladie, G. *Tetrahedron* **1980**, *36*, 227−237. (c) Ojima, I.; Yoshida, K.; Inaba, S.-i. *Chem. Lett.* **1977**, 429−432. (d) Akiyama, T.; Ishikawa, K.; Ozaki, S. *Synlett* **1994**, 275−276. (e) Sakito, Y.; Asami, M.; Mukaiyama, T. *Chem. Lett.* **1980**, 455−457. (f) Reetz, M. T.; Hullmann, M. *J. Chem. Soc., Chem. Commun.* **1986**, 1600−1602. (g) Guanti, G.; Riva, R. *Tetrahedron Lett.* **1995**, *36*, 3933−3936.

(10) For additions of chiral enolates to ketones, see: (a) Bartroli, J.; Turmo, E.; Belloc, J.; Forn, J. *J. Org. Chem.* **1995**, *60*, 3000−3012. (b) Judge, T. M. et al. *J. Am. Chem. Soc.* **1997**, *119*, 3627−3628. (c) Takagi, R.; Kimura, J.; Shinohara, Y.; Ohba, Y.; Takezono, K.; Hiraga, Y.; Kojima, S.; Ohkata, K. *J. Chem. Soc., Perkin Trans. 1* **1998**, 689−699. (d) Jacobson, I. C.; Reddy, G. P. *Tetrahedron Lett.* **1996**, *37*, 8263−8267. (e) Basavaiah, D.; Bharathi, T. K. *Tetrahedron Lett.* **1991**, *32*, 3417−3420. (f) Soloshonok, V. A.; Avilov, D. V.; Kukhar, V. P. *Tetrahedron* **1996**, *52*, 12433−12442.

(11) For chiral amino alcohol mediated enantioselective Reformatsky-type reactions with ketones, see: (a) Soai, K.; Oshio, A.; Saito, T. *J. Chem. Soc., Chem. Commun.* **1993**, 811−812. (b) Andrés, J. M.; Martín, Y.; Pedrosa, R.; Pérez-Encabo, A. *Tetrahedron* **1997**, *53*, 3787−3794. (c) Ojida, A.; Yamano, T.; Taya, N.; Tasaka, A. *Org. Lett.* **2002**, *4*, 3051−3054.

(12) Denmark, S. E.; Winter, S. B. D.; Su, X.; Wong, K.-T. *J. Am. Chem. Soc.* **1996**, *118*, 7404−7405.
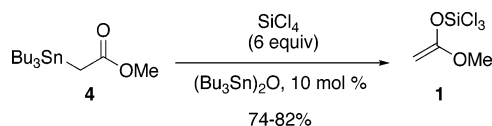
SCHEME 1

were to explore the scope of this reaction with regard to ketone partners and to design highly selective chiral Lewis base catalysts for this process. This report details in full our investigations of both the catalyzed and uncatalyzed additions of methyl trichlorosilyl ketene acetal to ketones.[13]

Results

1. Synthesis of Methyl Trichlorosilyl Ketene Acetal. Burlachenko and co-workers first described the preparation of methyl trichlorosilyl ketene acetal **1** by transmetalation of α-stannyl ester **4** with $SiCl_4$ (Scheme 2).[14] In Burlachenko's original report, stannyl ester **4** was obtained in low yield after fractional distillation at high temperature. A modification developed in these laboratories improved the preparation of the stannyl ester **4** and the procedure for the metathesis reaction.[12] The new procedure afforded **4** in higher yield and purity through purification by preparative HPLC.

SCHEME 2
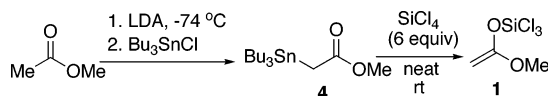
It was subsequently discovered, however, that the transmetalation step was not reproducible using the material purified by preparative HPLC. Depending on the batch, the complete consumption of **4** required hours to days. When **4** was further purified by vacuum distillation after column chromatography, the transmetalation proceeded to only 60% conversion even after 3 days.

We surmised that the decrease in the reaction rate with highly purified materials was likely the result of removing a catalytically active contaminant. To identify that component, the impurities removed during purification were subject to closer examination. A small amount of tributyltin methoxide was isolated from one run, and its influence on the reaction rate of transmetalation was investigated. In the presence of 5 mol % of this agent, the exchange was complete within minutes. Unfortunately, this reagent also caused the rapid decomposition of **1**.

We next investigated the use of a hindered tin oxide and selected commercially available and inexpensive bis-(tributyltin) oxide. Gratifyingly, as little as 10 mol % of $(Bu_3Sn)_2O$ was found to significantly accelerate the transmetalation without destroying the product (Scheme 3). The reaction was reproducibly complete within 4 h, and the trichlorosilyl ketene acetal **1** was obtained in consistently higher yields (74−82%).

(13) A preliminary account of this work has already appeared. Denmark, S. E.; Fan, Y. *J. Am. Chem. Soc.* **2002**, *124*, 4233−4235.

(14) Burlachenko, G. S.; Khasapov, B. N.; Petrovskaya, L. I.; Baukov, Y. I.; Lutsenko, I. F. *J. Gen. Chem. USSR (Engl. Transl.)* **1966**, *36*, 532−536.

SCHEME 3

2. Solvent Effects on the Uncatalyzed Aldol Addition. The optimization of the uncatalyzed aldol addition of **1** began by examination of the effect of solvent on the rate. The addition of **1** to acetophenone (**2a**) was examined in several solvents, and the results are summarized in Table 1. In noncoordinating solvents, such as methylene chloride and chloroform, the unpromoted reaction did not proceed at 0 °C (Table 1, entries 1 and 2). In coordinating solvents, such as acetonitrile, propionitrile, tetrahydrofuran, and diethyl ether, significant conversions (up to 46%) to product were observed by ^{1}H NMR analysis (Table 1, entries 3−6). Because only a negligible background reaction was seen in methylene chloride and chloroform, these two solvents were chosen for further study.

TABLE 1. Solvent Study of Uncatalyzed Aldol Addition

entry	solvent	conversion,[a] %
1	methylene chloride	2
2	chloroform	3
3	diethyl ether	8
4	tetrahydrofuran	18
5	acetonitrile	23
6	propionitrile	46

[a] Calculated on the basis of the ratio of integrated intensity of the methyl signal (Me*) in **5** and that of **2a**.

3. Survey of Lewis Base Promoter. 3.1. Survey of General Classes of Lewis Bases. To identify potential catalysts, a range of Lewis bases was investigated in the addition of **1** to **2a**. This survey was performed using 1 equiv of the Lewis base in CDCl₃, and the reaction progress was monitored by ^{1}H NMR spectroscopy. The conversions were calculated based on the ratio of integrated intensity of the methyl signal (Me*) in the trichlorosilyl aldolate **5** and that of **2a**. The results are summarized in Table 2.

Triphenylphosphine, DMF, pyridine, DMPU, and tetramethylthiourea showed little or no promoting ability (Table 2, compare entries 1−6). In contrast, DMSO, trimethylamine *N*-oxide, and HMPA were found to promote the reaction (Table 2, entries 7−9). In the presence of DMSO, the aldolate **5** (36%) was instantly formed upon mixing **1** with **2a** (Table 2, entry 7). However, the use of DMSO also resulted in the formation of many side products, and after 30 min, no further consumption of **2a** was observed. On the other hand, when trimethylamine *N*-oxide and HMPA were used, the reaction proceeded rapidly and cleanly.

3.2. Survey of *N*-Oxides. Because trimethylamine *N*-oxide demonstrated good promoting ability, the compatibility of different classes of *N*-oxides with **1** were next investigated. Aromatic amine *N*-oxides, trialkylamine *N*-oxides, and bis-*N*-oxides were examined in the addition

TABLE 2. Lewis Base Promoted Addition of 1 to 2a

entry	promoter	time, min	conv,[a] %
1	none	180	20
2	PPh₃	180	21
3	DMF	180	26
4	pyridine	180	35
5	DMPU	180	27
6	tetramethylthiourea	90	11
7	DMSO	30	36
8	trimethylamine *N*-oxide	10	70
9	HMPA	60	100

[a] Calculated on the basis of the ratio of integrated intensity of the methyl signal (Me*) in **5** and that of **2a**.

of **1** to **2a** in dichloromethane by variable-temperature ^{1}H NMR spectroscopy. The results are summarized in Table 3.

All of these *N*-oxides were found to promote the reaction. The aromatic amine *N*-oxides and trimethylamine *N*-oxide were compatible with **1**, and the reaction proceeded to completion (Table 3, entries 2−4). After the reaction was quenched with saturated aqueous NaHCO₃ solution, the corresponding *N*-oxide was recovered in yields greater than 80%. Among the aromatic amine *N*-oxides, pyridine *N*-oxide was significantly more reactive than 1,1′-biisoquinoline bis-*N*-oxides (Table 3, compare entries 2 and 4). *N*-Methylmorpholine *N*-oxide and quinuclidine *N*-oxide initiated the reaction at low temperature, but the reaction stalled and no further conversion was observed upon warming (Table 3, entries 5 and 6). Neither of these *N*-oxides could be recovered after quenching and workup of the reactions. Because pyridine *N*-oxide demonstrated superior promoting ability, it was chosen as the platform for further catalyst development.
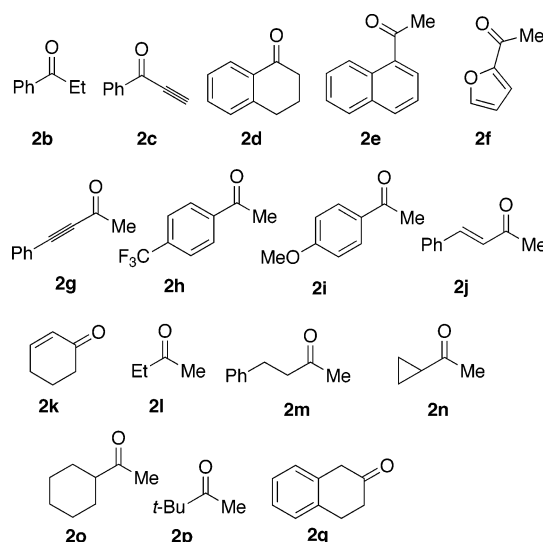
TABLE 3. Addition of 1 to Acetophenone Promoted by *N*-Oxides

entry	promoter	T, °C	time, min	conv,[a] %
1	none	−78	240	0
		−50	240	0
2	pyridine *N*-oxide	−78	70	37
		−50	50	97
3	trimethylamine *N*-oxide	−78	240	10
		−20	50	76
4	1,1′-biisoquinoline bis-*N*-oxide	−78	240	0
		−20	40	10
		0	150	100
5[b]	*N*-methylmorpholine *N*-oxide	−78	70	25
6[b]	quinuclidine *N*-oxide	−78	70	35

[a] Calculated on the basis of the ratio of integrated intensity of the methyl signal (Me*) in **5** and that of acetophenone. [b] No further conversion was observed upon warming.

4. Survey of Ketone Substrates. Before an extensive effort of developing a chiral catalyst was initiated, the scope of the reaction with regard to the ketone substrate was first established. A variety of structural types were

CHART 1

2b **2c** **2d** **2e** **2f**

2g **2h** **2i** **2j**

2k **2l** **2m** **2n**

2o **2p** **2q**

CHART 2

6 **7** **8**

9, R = Bn
10, R = mesityl   **11**

12

TABLE 4. Pyridine *N*-Oxide Catalyzed Additions of 1 to Ketones 2

entry	ketone	product	time, h	yield,[a] %
1	**2a**	**3a**	2	94
2	**2b**	**3b**	2	92
3	**2c**	**3c**	2	72
4	**2d**	**3d**	2	87
5	**2e**	**3e**	16	91
6	**2f**	**3f**	2	91
7	**2g**	**3g**	2	92
8	**2h**	**3h**	4	90
9	**2i**	**3i**	2	94
10	**2j**	**3j**	2	92
11	**2k**	**3k**	2	71
12	**2l**	**3l**	8	83
13	**2m**	**3m**	2	94
14	**2n**	**3n**	2	87
15	**2o**	**3o**	2	94
16	**2p**	**3p**	8	93
17	**2q**	**3q**	2	45

[a] Yields of analytically pure material.

TABLE 5. Chiral Phosphoramide Catalyzed Addition of 1 to 2a

catalyst	yield,[a] %	er[b]
none	0	
6	65	55.5/44.5
7	56	59.5/40.5
8	66	51.0/49.0
9	60	52.5/47.5
10	50	57.0/43.0
11	56	61.5/38.5
12	55	63.9/36.1

[a] Yields of chromatographically homogeneous material. [b] Determined by CSP-HPLC.

chosen with representatives in all basic structural classes (aromatic, heteroaromatic, olefinic, acetylenic, aliphatic (branched and linear)) as shown in Chart 1. The results of pyridine *N*-oxide catalyzed addition of **1** to these ketones are collected in Table 4.

These reactions proceeded smoothly with nearly all classes of ketone substrates. Good yields of the aldol products were obtained with aromatic (Table 4, entries 1–5, 8, and 9), heteroaromatic (Table 4, entry 6), olefinic (Table 4, entries 10 and 11), acetylenic (Table 4, entries 3 and 7), and aliphatic (Table 4, entries 12–16) ketones. The only low yield was obtained with 2-tetralone (**2q**), which afforded a 45% yield of the addition product **3q** and returned 45% of unreacted starting material, most likely from competitive enolization (Table 4, entry 17). The presence of multiple reaction sites did not interfere with the aldol addition; e.g., no conjugate addition products were observed for potential Michael acceptors

2c, **2g**, **2j** and **2k** (Table 4, entries 3, 7, 10, and 11). The steric encumbrance of the ketone substrate had a significant effect on the reaction rate: 1-acetonaphthone **2e** and pinacolone **2p** required 16 and 8 h at rt for completion, respectively (Table 4, entries 5 and 16). Nevertheless, high yields were obtained for these hindered ketones as well.

5. Survey of Chiral Phosphoramide Catalysts. The broad substrate generality of the transformation stimulated the search for a suitable chiral catalyst. Because HMPA is an effective catalyst for the addition of **1** to acetophenone, a range of available chiral phosphoramides were surveyed in this reaction first (Chart 2).[15] Phosphoramides derived from diamines with axial or central chirality were tested under a standard set of conditions of using 10 mol % of the catalysts, 0.2 M in CH$_2$Cl$_2$ at −24 °C. The results are summarized in Table 5.

Only modest enantioselectivities were observed with all of the chiral phosphoramides tested. Evidently, asymmetric induction is possible in this new aldol addition reaction with ketones. However, the minimal responses of enantioselectivities over a wide range of phosphoramide structures warranted the development of a new class of chiral Lewis bases.

(15) Denmark, S. E.; Su, X.; Nishigaichi, Y.; Wong, K.-T.; Coe, D. M.; Winter, S. B. D.; Choi, J.-Y. *J. Org. Chem.* **1999**, *64*, 1958–1967.

6. Survey of Chiral Pyridine *N*-Oxide Catalysts. Because pyridine *N*-oxide was a highly effective catalyst for the addition of **1** to a variety of ketones, it was chosen as a second platform for the development of chiral catalysts. To assay the effectiveness of different chiral elements in achieving enantioselection, a collection of *N*-oxides possessing either central or axial chiral elements were surveyed in the addition of **1** to **2a** (Chart 3). For example, the camphor-derived reagent **13** has been employed effectively in various reactions.[16] Accordingly, **14** was prepared to provide a direct comparison between monomeric and dimeric *N*-oxides. Bis-*N*-oxides **15** and **16** have been used previously in the related addition of allyltrichlorosilane to aldehydes;[17] therefore, they were chosen as the representative catalysts that embody axial chirality.[18] Another class of bis-*N*-oxides was inspired by the work of Bolm, who combined both central and axial chiral elements in the bipyridyl precursor for **17** bearing stereocenters in the 6,6′-positions.[19]
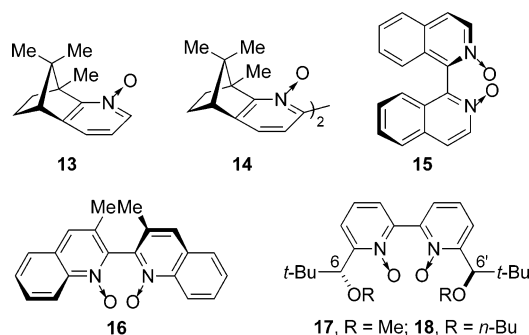
CHART 3

13   **14**   **15**

16   **17**, R = Me; **18**, R = *n*-Bu

TABLE 6. Chiral *N*-Oxide Catalyzed Addition of 1 to 2a

| entry	catalyst	yield,[a] %	er[b]
1	**13**	55	51.5/48.5
2	**14**	15	50.2/49.8
3	**15**	45	72.5/27.5
4	**16**	39	63.0/37.0
5	**17**	92	77.4/22.6
6	**18**	94	81.9/18.1

[a] Yields of chromatographically homogeneous material. [b] Determined by CSP-SFC.

Orienting reactions were performed under a standard set of conditions: 10 mol % catalyst loading, 0.2 M concentration in CH_2Cl_2 at 0 °C and 2.5 h reaction time. The yields and enantioselectivities are summarized in Table 6. Both the mono-*N*-oxide **13** and bis-*N*-oxide **14** derived from (+)-(*R*)-camphor afforded disappointing

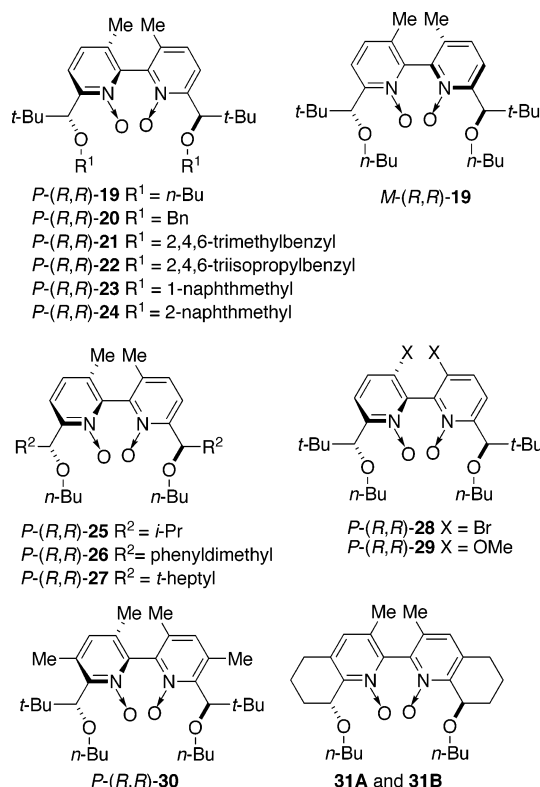(16) Chelucci, G.; Murineddu, G.; Pinna, G. A. *Tetrahedron: Asymmetry* **2004**, *15*, 1373−1389.

(17) Nakajima, M.; Saito, M.; Shiro, M.; Hashimoto, S.-i. *J. Am. Chem. Soc.* **1998**, *120*, 6419−6420.

(18) (a) Malkov, A. V.; Kocovsky, P. *Curr. Org. Chem.* **2003**, *7*, 1737−1757. (b) McCarthy, M.; Guiry, P. J. *Tetrahedron* **2001**, *57*, 3809−3844.

(19) (a) Bolm, C.; Ewald, M.; Zehnder, M.; Neuburger, M. A. *Chem. Ber.* **1992**, *125*, 453−458. (b) Bolm, C.; Ewald, M.; Felder, M.; Schlingloff, G. *Chem. Ber.* **1992**, *125*, 1169−1190.

results both in terms of reactivity and selectivity (Table 6, entries 1 and 2). 1,1′-Biisoquinoline and 2,2′-biquinoline derived bis-*N*-oxides **15** and **16** could effectively catalyze the addition of **1** to acetophenone albeit with only modest enantioselectivities (Table 6, entries 3 and 4). Gratifyingly, both **17** and **18** provided improved enantioselectivities, affording an enantiomeric ratio of 82/18 in nearly quantitative yield (Table 6, entries 5 and 6).

7. Development of Chiral *N*-Oxide Catalysts Possessing Both Central and Axial Chirality. The high reactivity and encouraging selectivity observed with bis-*N*-oxides **17** and **18** stimulated further optimization of this class of catalysts. However, unlike **15** or **16**, the chiral axis in this class is configurationally labile. When complexed to enolate **1**, two atropisomeric diastereomers can be formed (Scheme 4, **A** and **B**), which could lead to compromised enantioselectivity.

SCHEME 4

A   **B**
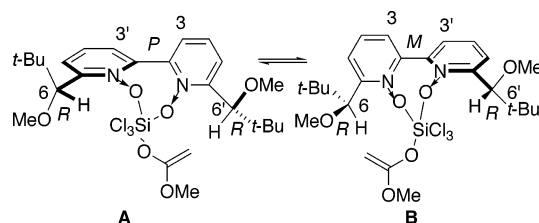
Results from low-temperature ¹H NMR spectroscopic analysis of the complex **17·1** indicated rapid interconversion between different stereoisomers of **17·1**: only one set of broadened signals was observed at −60 °C. Clearly, under the conditions for the aldol addition (−20 °C), the atropisomerism of complex **17·1** is not controlled. Therefore, modified catalysts were designed in which the configuration of the chiral axis is fixed. This is most easily accomplished by the introduction of methyl groups at the 3,3′-positions.

To accomplish the synthesis of this new class of bipyridine bis-*N*-oxides possessing fixed elements of both central and axial chirality, a new method of preparation had to be developed and is described below.[20] To establish a structure/enantioselectivity relationship, a collection of bis-*N*-oxides (*P*)-(*R*,*R*)-**19**−**31** was designed and synthesized (Chart 4). Catalysts (*P*)-(*R*,*R*)-**19-24** were prepared to study the steric effects of the ether protecting group R¹, whereas catalysts (*P*)-(*R*,*R*)-**25**−**27** were prepared to study the steric effects of the substituent R². The electronic effects of ring substituents on catalytic activity were investigated by comparing the enantioselectivities of (*P*)-(*R*,*R*)-**28** and (*P*)-(*R*,*R*)-**29**. Catalysts (*P*)-(*R*,*R*)-**30**, **31A**, and **31B** were prepared to investigate the effect of changing dihedral angle O−C(6′)−C(6)−N on the enantioselectivity. The reactions were performed under a standard set of conditions: 10 mol % catalyst, 0.2 M concentration in CH_2Cl_2 at −20 °C and 12 h reaction time. The yields and enantioselectivities are summarized in Table 7.

Improved enantioselectivity was observed with the *P*-configured bis-*N*-oxide (*P*)-(*R*,*R*)-**19** (compare Table 7, entry 1, and Table 6, entry 6). Interestingly, the diaster-

(20) The syntheses of the various bis *N*-oxides employed in this work constitutes a major effort that will be described separately. Denmark, S. E.; Fan, Y. Manuscript in preparation.

CHART 4

P-(R,R)-**19** R¹ = n-Bu
P-(R,R)-**20** R¹ = Bn
P-(R,R)-**21** R¹ = 2,4,6-trimethylbenzyl
P-(R,R)-**22** R¹ = 2,4,6-triisopropylbenzyl
P-(R,R)-**23** R¹ = 1-naphthmethyl
P-(R,R)-**24** R¹ = 2-naphthmethyl

M-(R,R)-**19**

P-(R,R)-**25** R² = i-Pr
P-(R,R)-**26** R²= phenyldimethyl
P-(R,R)-**27** R² = t-heptyl

P-(R,R)-**28** X = Br
P-(R,R)-**29** X = OMe

P-(R,R)-**30**

31A and **31B**

TABLE 7. Chiral Bis-*N*-oxide Catalyzed Addition of 1 to 2a

entry	catalyst	yield,[a] %	er,[b] S/R
1[d]	P-(R,R)-**19**	90	87.1/12.9
2	P-(R,R)-**19**	94	91.3/8.7[c]
3	M-(R,R)-**19**	89	29.6/71.4
4	P-(R,R)-**20**	89	91.0/9.0
5	P-(R,R)-**21**	91	93.5/6.5
6	P-(R,R)-**22**	64	80.0/20.0
7	P-(R,R)-**23**	88	87.0/13.0
8	P-(R,R)-**24**	91	49.5/50.5
9	P-(R,R)-**25**	93	82.0/18.0
10	P-(R,R)-**26**	90	89.9/10.1
11	P-(R,R)-**27**	87	73.5/26.5
12	P-(R,R)-**28**	32	80.5/19.5
13	P-(R,R)-**29**	95	86.0/14.0
14	P-(R,R)-**30**	93	86.0/14.0
15[e]	31A	92	62.0/38.0
16[e]	31B	94	47.5/52.5

[a] Yields of chromatographically homogeneous material. [b] Determined by CSP-SFC. [c] Absolute configuration *S* by correlation to the literature data.[21] [d] Reaction performed at 0 °C. [e] Configuration of the chiral axis unknown.

eomeric *M*-isomer, (*M*)-(*R,R*)-**19** catalyzed the aldol reaction in high yield but afforded the enantiomer of **3a** with modest selectivity (Table 7, entry 3). Thus, it is clear that in these catalysts, the configuration of the chiral axis dominates the sense of the asymmetric induction while the 6,6′-stereocenters play a secondary role. Furthermore, in (*P*)-(*R,R*)-**19**, the sense of asymmetric induction from the chiral centers matches with that from the chiral axis

while in (*M*)-(*R,R*)-**19** they are mismatched. The enantioselectivity with (*P*)-(*R,R*)-**19** could be enhanced by simply carrying out the reaction at −20 °C for 12 h (Table 7, entries 1 and 2). From the sign of optical rotation of the product ($[\alpha]^{24}_D$ −5.62 (EtOH)), the absolute configuration of **3a** was deduced to be *S* (lit.[21] er *S/R* 79/31, $[\alpha]^{24}_D$ −4.96 (EtOH)).

The correlation between the enantioselectivity and the size and shape of substituents on 6,6′-stereocenters was further investigated by systematic structural variations. With regard to the choice of R¹, the benzyl group was nearly as effective as the *n*-butyl group in terms of rate and selectivity (compare Table 7, entries 2 and 4), and the enantioselectivity was further increased to 93.5/6.5 er when the more sterically hindered mesityl group was used (Table 7, entry 5). However, further increase in the size of this group to triisopropylbenzyl led to diminished reactivity and selectivity (Table 7, entry 6). The dramatic difference between the results from 1-naphthmethyl and 2-naphthmethyl substituents was puzzling (Table 7, entries 7 and 8) and suggested that asymmetric induction from the stereocenter with 2-naphthmethyl substituent is mismatched with that from the chiral axis. With respect to the choice of R², the *tert*-butyl group was optimal (Table 7, entry 2). A significant decrease in enantiomeric ratio (from 92/8 to 82/18) was observed when changing from the *tert*-butyl to the smaller isopropyl group (compare entries 2 and 9). On the other hand, whereas a slight increase in the size of the R² group had only a negligible influence (Table 7, entry 10), the sterically demanding *tert*-heptyl substituent in catalyst (*P*)-(*R,R*)-**27** resulted in a drastic decrease in selectivity (Table 7, entry 11), indicating that the influence from the 6,6′-stereocenters becomes competitive with the chiral axis.

The activity of the catalyst decreased significantly when a bromine atom was attached at the 3,3′-position (Table 7, entry 12), whereas no significant change in reactivity observed with a methoxy group at this position (Table 7, entry 13). Apparently, the electron-withdrawing property of the bromine decreases the basicity of the catalyst and its ability to activate **1**.

The orientation of the groups at the 6,6′-stereocenter is another key factor in defining the chiral environment around the reaction field. The influence of the conformational variations were investigated by restricting the single bond rotation between the 6,6′-center and the pyridine ring (Figure 1). Catalyst (*P*)-(*R,R*)-**30** was designed to rotate the butoxy group away from the *N*-oxide unit by the steric repulsion between the 5-methyl and the *tert*-butyl groups. In a complementary fashion, catalysts **36A** and **36B** were designed to lock the butoxy group nearer to the *N*-oxide unit through constriction in a ring.
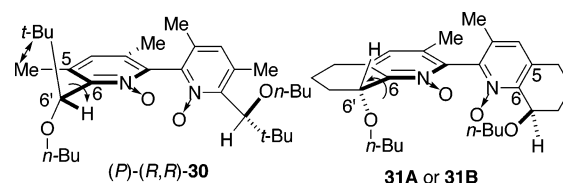

(*P*)-(*R,R*)-**30**   **31A** or **31B**

FIGURE 1. Design of catalyst for conformational control.

(21) Basavaiah, D.; Bharathi, T. K. *Tetrahedron Lett.* **1991**, *32*, 3417−3420.

TABLE 8. Bis-*N*-oxide (*P*)-(*R,R*)-19 Catalyzed Additions of 1 to Ketones

entry	ketone	product	yield,[a] %	er[b]
1	**2a**	**3a**	96	91.2/8.7
2	**2b**	**3b**	90	90.3/9.7[c]
3	**2c**	**3c**	89	93.1/6.9
4	**2d**	**3d**	90	90.1/9.9
5	**2e**	**3e**	89	77.9/22.1
6	**2f**	**3f**	87	74.3/25.7
7	**2g**	**3g**	94	67.6/32.4
8	**2h**	**3h**	91	88.0/12.0
9	**2i**	**3i**	94	83.9/16.1
10	**2j**	**3j**	87	55.4/44.6
11	**2k**	**3k**	86	53.9/46.1
12	**2l**	**3l**	84	66.1/33.9
13	**2m**	**3m**	97	67.5/32.5
14	**2n**	**3n**	84	60.1/39.9
15	**2o**	**3o**	91	66.0/34.0
16	**2p**	**3p**	87	71.5/28.5

[a] Yields of analytically pure material. [b] Determined by CSP-SFC. [c] Absolute configuration *S* by correlation to the literature (see the Supporting Information).

A slight decrease in selectivity was observed with catalyst (*P*)-(*R,R*)-**30** (Table 7, entry 14), indicating the importance of positioning the ether side chain close to the reaction center. On the other hand, the disappointing results from both atropisomers **31A** and **31B** suggested the possibility that new unselective reaction pathways become significant upon imposing severe steric interactions around the silicon center (Table 7, entries 15 and 16).

8. Chiral Bis-*N*-oxide-Catalyzed Additions to Ketones. The scope of asymmetric additions of **1** to various ketones found in Chart 2 was examined with catalyst (*P*)-(*R,R*)-**19**. The reactions were performed on a 2.0 mmol scale (0.2 M) at −20 °C for 12 h, and the results are summarized in Table 8.

The superior catalytic activity of (*P*)-(*R,R*)-**24** was demonstrated in the aldol addition of **1** to every class of nonactivated ketones. All reactions proceeded cleanly, and high yields of the aldol products were obtained for all of the ketone substrates The enantioselectivity, however, was found to be highly dependent on the structure of the ketone. Aromatic ketones generally gave good enantioselectivities (Table 8, entries 1−4). The highest enantioselectivity (93.1/6.9 er) was obtained with 1-phenyl-2-propyn-1-one **2c** wherein the sizes of the two flanking groups are the most different (Table 8, entry 3). Minimal but noticeable erosion in the enantioselectivity was observed when the difference between the size of two flanking groups decreases: from 93.1/6.9 er for acetylene (**2c**) to 91.2/8.7 er for methyl (**2a**) and to 90.3/9.7 er for ethyl group (**2b**) (Table 8, entries 1−3). In this regard, the modest selectivity seen with 1-aceto-naphthone (**2e**) (Table 8, entry 5) was surprising, hinting that the size of aromatic group also has a significant influence on the enantioselectivity.

A noticeable electronic effect was manifested in the lower selectivities for both the electron-poor and electron-

rich ketones (Table 8, entries 1, 8, and 9). Accordingly, the lower selectivity observed for furyl methyl ketone might be due to the electron-rich nature of the furyl substituent (Table 8, entry 6).
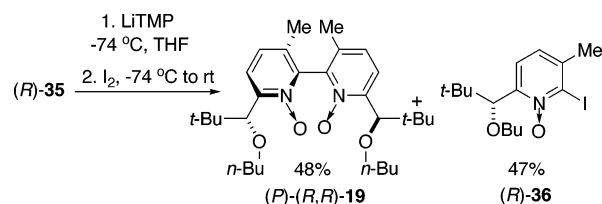
9. Catalyst Synthesis. 9.1. Synthesis of Bis-*N*-oxide (*P*)-(*R,R*)-19. The chiral bis-*N*-oxides shown in Chart 4 were synthesized by direct, diastereoselective dimerization of the corresponding monomeric chiral *N*-oxide. As a representative example, the synthesis of (*P*)-(*R,R*)-**19** is described herein (the syntheses of other catalysts will be reported separately).[20] The synthesis of (*P*)-(*R,R*)-**19** began with the preparation of pyridyl ketone **32** by trapping of 5-methyl-2-pyridyllithium with excess pivaloyl chloride (Scheme 5). Subsequent enantioselective reduction of **32** using (−)-(Ipc)$_2$BCl provided pyridyl alcohol (*R*)-**33** in good yield, albeit after long reaction time. The enantiomeric ratio (*R/S*, 97.8/2.2) was determined on the corresponding trifluoroacetate derivative (by CSP-GC) and the absolute configuration was determined by X-ray crystallographic analysis of complex of bis-*N*-oxide with silicon tetrachloride (vide infra). The formation of the butyl ether (*R*)-**34** required the use of a 6-fold excess of potassium hydride and *n*-butyl bromide. Subsequent oxidation of (*R*)-**34** to (*R*)-**35** proceeded uneventfully using *m*-CPBA.

SCHEME 5
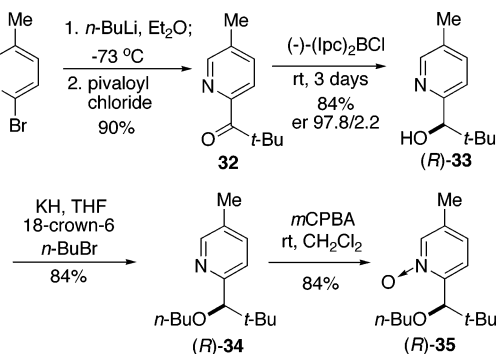
When (*R*)-**35** was lithiated with LiTMP and treated with iodine, the bis-*N*-oxide (*P*)-(*R,R*)-**19** was obtained in 48% yield along with a 47% yield of iodide (*R*)-**36** (Scheme 6). Interestingly, the *P*-configured atropisomer was produced with a diastereoselectivity greater than 20/1. The configuration of the chiral axis was determined by X-ray crystallographic analysis of the complex (*P*)-(*R,R*)-**19**·SiCl$_4$.

SCHEME 6

9.2. Synthesis of Bis-*N*-oxide (*M*)-(*R,R*)-19. Because (*P*)-(*R,R*)-**24** was formed almost exclusively in the dimerization, it was necessary to employ a reduction/reoxidation sequence for the preparation of (*M*)-(*R,R*)-**19** (Scheme 7). Reduction of *N*-oxide (*P*)-(*R,R*)-**19** with zinc powder provided a good yield of bipyridine (*R,R*)-**37**. Without the

N-oxide unit, the chiral axis in this compound is configurationally labile. Oxidation of (*R*,*R*)-**37** afforded a mixture of two atropisomers in a (*P*)-(*R*,*R*)-**19**/(*M*)-(*R*,*R*)-**19** ratio of 2.5/1. These two diastereomeric atropisomers were separated by silica gel column chromatography, and the minor diastereomer could be isolated and characterized.

SCHEME 7
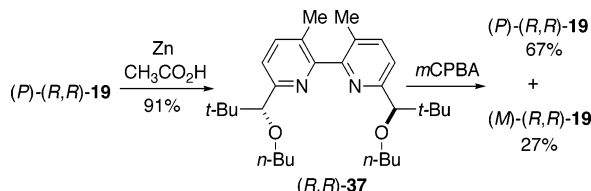
10. Structural Studies. 10.1. Preparation and X-ray Structural Analysis of Complex (*P*)-(*R*,*R*)-**19**·SiCl$_4$.

Because structural information on the coordination geometry of the bis-*N*-oxide/silicon complex is crucial for understanding the origin of enantioselection and optimization of selectivity, we set out to obtain a single-crystal X-ray structure of the bis-*N*-oxide/trichlorosilyl ketene acetal complex (*P*)-(*R*,*R*)-**19·1**. After extensive experimentation, conditions for growing single crystals were obtained by diffusing diethyl ether to a 1/1 mixture of (*P*)-(*R*,*R*)-**19** and **1** in methylene chloride at −20 °C. Surprisingly, the material that crystallized was not the expected complex, but X-ray analysis revealed it to be (*P*)-(*R*,*R*)-**19**·SiCl$_4$ (Scheme 8). Apparently, this complex was generated from the disproportionation of **1** or (*P*)-(*R*,*R*)-**19·1** and crystallized out of the mixture. Curiously, when an equivalent amount of SiCl$_4$, instead of trichlorosilyl ketene acetal **1**, was used for the crystal growth under otherwise identical conditions, an amorphous powder was formed instead. In sharp contrast, the single crystals of the complex (*P*)-(*R*,*R*)-**19**·SiCl$_4$ could be grown out of a solution of (*P*)-(*R*,*R*)-**19** and **1** reproducibly.

SCHEME 8
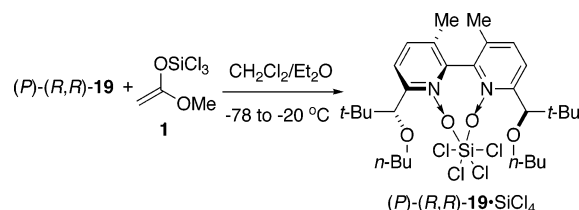
10.2. VT NMR Study on Bis-*N*-oxide/Silicon Complex.

To determine if the trichlorosilyl ketene acetal **1** disproportionates under the conditions for the aldol reaction, a variable-temperature NMR study was undertaken on the complexes of (*P*)-(*R*,*R*)-**19** with SiCl$_4$ and with **1**. The characteristic signals from their ¹H NMR and ²⁹Si NMR spectra and those of the free ligand are listed in Table 9. In the presence of 1.0 equiv of SiCl$_4$, the NMR signals for (*P*)-(*R*,*R*)-**19** were replaced with a new set of signals indicating that complexation was taking place. We believe that the new species formed is (*P*)-(*R*,*R*)-**19**·SiCl$_4$ on the basis of the ²⁹Si NMR chemical shift (−167) which is squarely in the hexacoordinate region for silicon[22] and also by the fact that the symmetry of the ligand is preserved. When bis-*N*-oxide (*P*)-(*R*,*R*)-**19** was

TABLE 9. Characteristic NMR Resonances of (*P*)-(*R*,*R*)-19 and Its Silicon Complexes

sample	T, °C	H*, ppm	²⁹Si, ppm
(*P*)-(*R*,*R*)-**19**	−78	4.85	
	−40	4.90	
	−20	4.93	
(*P*)-(*R*,*R*)-**19** + SiCl$_4$	−78	5.62	
	−40	5.75	
	−20	5.75	−167
(*P*)-(*R*,*R*)-**19** + **1**	−78	5.61, 5.82 (5.62)[a]	
	−40	5.68, 5.89 (5.75)[a]	
	−20	5.68, 5.89 (5.75)[a]	−163 −167[a]

[a] Signals from (*P*)-(*R*,*R*)-**19**·SiCl$_4$.

mixed with 1.0 equiv of trichlorosilyl ketene acetal **1**, the NMR spectrum revealed the presence of the complex (*P*)-(*R*,*R*)-**19**·SiCl$_4$ and another species. We conclude that this new species is (*P*)-(*R*,*R*)-**19·1** again on the basis of its ²⁹Si NMR chemical shift (−163) and the appearance of two, diasterotopic methine protons, H*, which indicate the asymmetry of the complex. The ratio of complex (*P*)-(*R*,*R*)-**19·1** to (*P*)−(*R*,*R*)-**19**·SiCl$_4$ was calculated on the basis of the integrated intensity of the signal from the benzylic proton and was found to be dependent on temperature, varying from 2.5/1 at −78 °C to 0.31 /1 at −40 °C, to 0.15/1 at −20 °C, which indicated that complex (*P*)-(*R*,*R*)-**19**·SiCl$_4$ is favored at higher temperature.

10.3. Structural Features of Complex (*P*)-(*R*,*R*)-19·SiCl$_4$.

Although all attempts to obtain a crystal structure of the complex (*P*)-(*R*,*R*)-**19·1** were thwarted by the disproportionation process, the silicon tetrachloride complex (*P*)-(*R*,*R*)-**19**·SiCl$_4$ nonetheless provided a wealth of structural information. The Chem-3D representation of this complex is shown in Figure 2, and selected bond lengths and bond angles are listed in Table 10.[23]

The complex (*P*)-(*R*,*R*)-**19**·SiCl$_4$ has an octahedral geometry with only slight distortion; all of the *cis* bond angles are close to 90° (84.6−92.6°), whereas *trans* angles are greater than 170° (175.7−176.9°). As expected, the bis-*N*-oxide is chelated to the silicon unit to form a strongly twisted seven-membered ring (Figure 3A). The chiral axis is *P*-configured (Figure 3B), and two pyridine rings are significantly distorted from orthogonality with a dihedral angle of 73.2°. The *tert*-butyl groups at the 6,6′-centers are disposed to minimize steric interaction resulting in a C(23)−C(22)−C(10)−N(2) dihedral angle of close to 90° (Figure 3C). Finally, the ether side chains at the 6,6′-stereogenic centers have an extended conformation, presumably to minimize repulsion between the

(22) Kennedy, J. D.; McFarlane, W. In *Multinuclear NMR*; Mason, J., Ed.; Plenum Press: New York, 1987; Chapter 11.
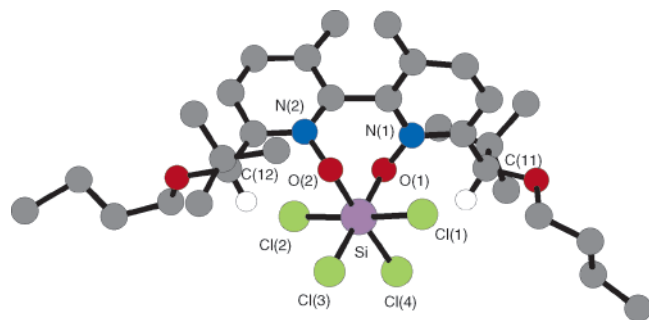
FIGURE 2. Chem-3D representation of (P)-(R,R)-**19**·SiCl$_4$ complex (hydrogens omitted for clarity, except HC(11) and HC(12)).

TABLE 10. Selected Bond Lengths and Bond Angles of Complex (P)-(R,R)-**19**·SiCl$_4$

bond length (Å)		bond angles (deg)	
Si−Cl(1)	2.176	Cl(1)−Si−Cl(2)	176.5
Si−Cl(2)	2.185	O(1)−Si−Cl(3)	175.7
Si−Cl(3)	2.199	O(2)−Si−Cl(4)	176.9
Si−Cl(4)	2.194	Cl(1)−Si−Cl(3)	91.7
Si−O(1)	1.839	Cl(1)−Si−Cl(4)	91.4
Si−O(2)	1.839	Cl(2)−Si−Cl(3)	91.2
O(1)−N(1)	1.353	Cl(2)−Si−Cl(4)	90.7
O(2)−N(2)	1.364	O(1)−Si−O(2)	91.5
		O(1)−Si−Cl(1)	92.6
		O(1)−Si−Cl(2)	84.6
		O(2)−Si−Cl(1)	85.5
		O(2)−Si−Cl(2)	92.3
		O(1)−Si−Cl(4)	88.2
		O(2)−Si−Cl(3)	87.9
		Si−O(1)−N(1)	119.5
		Si−O(2)−N(2)	118.7

N−O and C−O dipoles and to minimize the steric interaction with both the *tert*-butyl group and the cis chloride (Figure 3A and C).

It is noteworthy that the average length of the Si−Cl bonds that oppose the *N*-oxide ligand (2.197 Å) is 0.017 Å longer than those that oppose the other chloride ligands (2.180 Å). This difference indicates that the *N*-oxide ligand has a stronger structural trans effect (STE)[24] than that of chloride (Table 10).

Discussion

1. Bis(trialkyltin) Oxide Catalyzed Metathesis Reaction. The bis(tributyltin) oxide catalyzed metathesis provided a reliable method for the preparation of methyl trichlorosilyl ketene acetal **1**. Consideration of the Lewis basicity of bis(tributyltin) oxide[25] leads to the following working hypothesis (Scheme 9). The initial step in the proposed catalytic cycle involves activation of the weak Lewis acid SiCl$_4$ by bis(tributyltin) oxide. Thus, upon binding one or two (Bu$_3$Sn)$_2$O molecules, ionization

(23) The crystallographic coordinates of (P)-(R,R)-**19**·SiCl$_4$ have been deposited with the Cambridge Crystallographic Data Centre; deposition no. CCDC 241716. These data can be obtained free of charge via www.ccdc.cam.ac.uk/conts/retrieving.html (or from the Cambridge Crystallographic Data Centre, 12 Union Road, Cambridge CB2 1EZ, U.K.; fax: (+44) 1223-336-033; deposit@ccdc.cam.ac.uk).

(24) For reviews on trans effects, see: (a) Coe, B. J.; Glenwright, S. J. *Coord. Chem. Rev.* **2000**, *203*, 5−80. (b) Shustorovich, E. M.; Porai-Koshits, M. A.; Buslaev, Y. A. *Coord. Chem. Rev.* **1975**, *17*, 1−98.

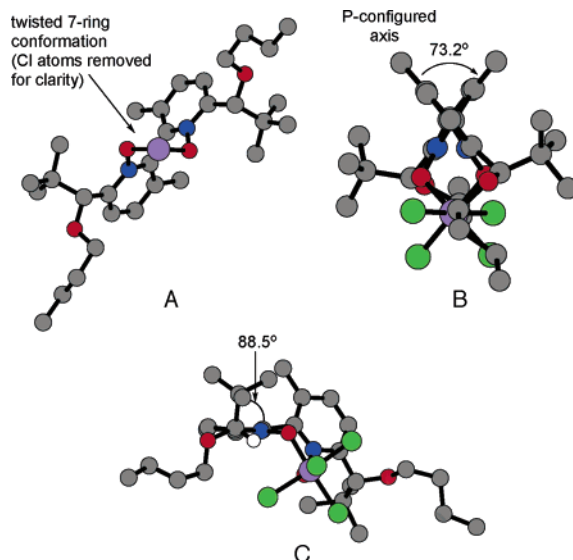(25) Rake, B.; Muller, P.; Roesky, H. W.; Uson, I. *Angew. Chem., Int. Ed.* **1999**, *38*, 2050−2051.

FIGURE 3. Global structure features of complex (P)-(R,R)-**19**·SiCl$_4$.

of chloride occurs and a cationic silicon species **i** is generated. It is reasonable that transmetalation of stannyl acetate **4** with this species is more facile than with SiCl$_4$ due to the enhanced Lewis acidity of the siliconium ion. Thus, trichlorosilyl ketene acetal **1** and byproduct tributyltin chloride are generated through a hexacoordinate cationic intermediate **ii**.

SCHEME 9
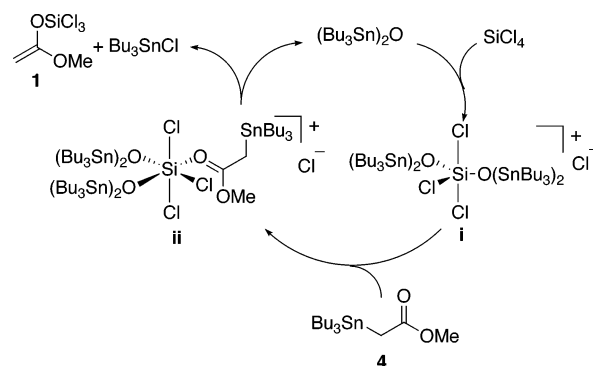
2. Pyridine *N*-Oxide Catalyzed Aldol Additions. Whereas the uncatalyzed aldol addition of **1** to acetophenone proceeds only slowly at room temperature, in the presence of a strongly ionizing Lewis base, such as HMPA or pyridine *N*-oxide,[26] the aldol addition takes place even at −78 °C. Furthermore, the pyridine *N*-oxide catalyzed addition tolerates a wide range of structural variations on the ketone acceptor. Excellent yields of β-tertiary hydroxy ester products can be obtained from aromatic, olefinic, acetylenic, and aliphatic ketones. Such a striking magnitude of rate acceleration and general substrate scope are synthetically useful and mechanistically intriguing.

Common ion effects of chloride on the related phosphoramide-catalyzed aldol addition of cyclohexanone-derived trichlorosilyl enolate to benzaldehyde revealed

(26) Bassindale, A. R.; Stout, T. *Tetrahedron Lett.* **1985**, *26*, 3403−3406.

that the origin of Lewis base catalysis in this type of aldol reaction stems from ionization of a chloride and reaction via a penta- or hexacoordinate siliconium ion.[27] Kinetic measurements[27a] indicated that two molecules of Lewis base are involved in the carbon–carbon bond-forming transition structure, whenever it is sterically accessible. It is reasonable that a similar mechanism might be operating in the additions of **1** to ketones. Thus, a hypothetical catalytic cycle can be drawn for the pyridine *N*-oxide catalyzed aldol additions of **1** to ketones (Scheme 10).

SCHEME 10
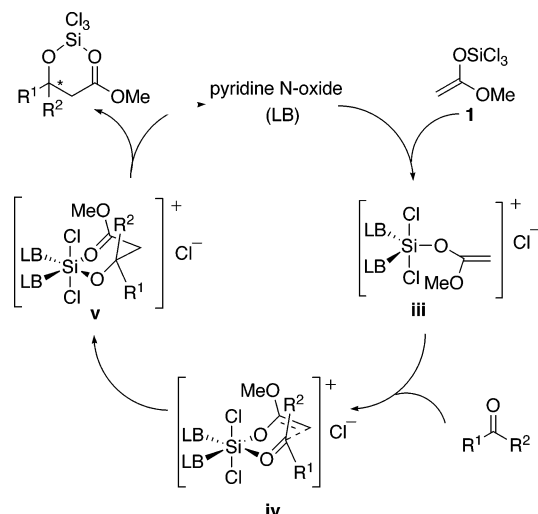
The binding of two pyridine *N*-oxide molecules to **1** leads to ionization of chloride and generates a cationic silyl enolate **iii**. The enhanced electrophilicity of **iii** overrides the steric encumbrance that attends the complexation of a ketone, and a ternary complex **iv** of **1**, the *N*-oxide, and the ketone is formed. By analogy to previous aldol reaction of trichlorosilyl enolates, the polarization of electron density upon complexation provides a dual activation of the reaction components. According to the Gutmann analysis,[28] the electron density which is drawn away from the carbonyl group (resulting in electrophilic activation of the ketone acceptor) is distributed to the other substituents in the formation of 3-center-4-electron bonds.[29] Thus, the enoxy fragment is nucleophilically activated, and the aldol addition proceeds via complex **iv**. After aldolization, a carboxylic ester moiety is generated, and the internal coordination of this group to the trichlorosilyl unit in **v** likely facilitates the release of pyridine *N*-oxide catalyst and completes the catalytic cycle.

3. The Origin of Enantioselectivity in Chiral Bis-*N*-oxide-Catalyzed Addition. 3.1. Mechanistic Hypotheses. The enantioselectivity observed with the chiral *N*-oxide catalysts employed here is highly dependent on the structure of the ketone. With aromatic ketones, enantiomeric ratios of up to 93.5/6.5 were obtained whereas with aliphatic and olefinic ketones the reactions were not selective. Clearly, high levels of enantioselectivity are only obtainable when the two groups flanking the carbonyl moiety are sterically and electronically differentiated.

To understand the origin of enantioselectivity observed in these reactions and to aid in the design and development of new catalysts capable of inducing higher levels of selectivity we turned to computational modeling. For this analysis it is a priori assumed that the reaction takes place through a ternary, cationic complex of the trichlorosilyl ketene acetal (**1**), a bis *N*-oxide catalyst, and a ketone as outlined in Scheme 10. Although the kinetic details of this proposed catalytic cycle are not known, it is also proposed that complexation of the ketone to the cationic complex **iii** is rapidly reversible, i.e., that the reaction is under Curtin–Hammett control,[30] with aldolization being turnover limiting. The observation of a natural abundance ^{13}C kinetic isotope effect at the carbonyl carbon in the reaction with aldehydes suggested that our assumption of rate-limiting aldolization is correct.[31] Under this assumption, the energies of the diastereomeric transition states are stereodetermining and the ground state energies of any intermediate complexes are not considered. Although a mechanism involving an open transition-state structure cannot be completely ruled out, consideration of the similarity between these reactions and those of **1** with aldehydes[12a] led us to propose a similar closed transition-state structure.

3.1. Limiting Structures of Silicon Complexes: Hypervalent Bonding. From the three reaction components, five limiting, diastereomeric, hexacoordinate, cationic complexes can be constructed that contain the cis relationship between the ketone and ketene acetal necessary for aldolization (Figure 4). To identify the location of the substituents, the equatorial plane is defined by the silicon and ligand oxygen atoms. Three basic families of cis complexes can be identified, diequatorial (**vi**), equatorial ketone–axial ketene acetal (**vii/viii**), and axial ketone–equatorial ketene acetal (**ix/x**). When the axial positions are occupied by a ligand other than chloride, the remaining equatorial positions are no longer homotopic, thus forming sets of diastereomeric complexes.

When silicon expands its coordination sphere to form an octahedral complex it does so by using two of its p-orbitals in hypervalent, 3-center-4-electron bonding and the remaining p-orbital and s-orbital hybridize to form two sp-hybrids (Figure 5).[32] These are lower in energy than the two hypervalent p-orbitals and engage in more "normal covalent bonding". Thus, the silicon atom is formally sp-hybridized. The hypervalent orbitals, created by three orbital overlap, possess a nonbonding orbital as their HOMO, placing most of the electron density on the external ligands. These positions are naturally preferred by the more electronegative substituents.[32] The two sp-hybrids, being lower in energy and rich in s-character,[33] are preferred by electropositive substituents with lower

(27) (a) Denmark, S. E.; Pham, S. M. *Helv. Chim. Acta* **2000**, *83*, 1846–1853. (b) Denmark, S. E.; Su, X.; Nishigaichi, Y. *J. Am. Chem. Soc.* **1998**, *120*, 12990–12991.

(28) Gutmann, V. *The Donor–Acceptor Approach to Molecular Interactions*; Plenum Press: New York, 1978; pp 12–14.

(29) Curnow, O. J. *J. Chem. Educ.* **1998**, *75*, 910–915.

(30) Seeman, J. I. *Chem. Rev.* **1983**, *83*, 83–134.

(31) Pham, S. M. Ph.D. Thesis; University of Illinois, Urbana–Champaign, 2002.

(32) Tandura, S. N.; Voronkov, M. G.; Alekseev, N. V. *Top. Curr. Chem.* **1986**, *113*, 99–189.

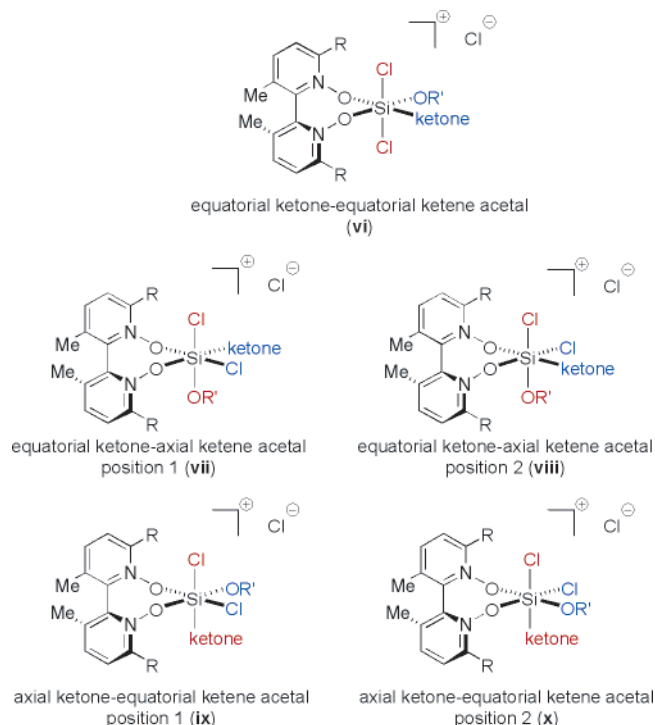(33) Bent, H. A. *Chem. Rev.* **1961**, *61*, 275–311.

FIGURE 4. Five reactive hexacoordinate complexes of a ketone with **1** and a chiral bis-*N*-oxide.
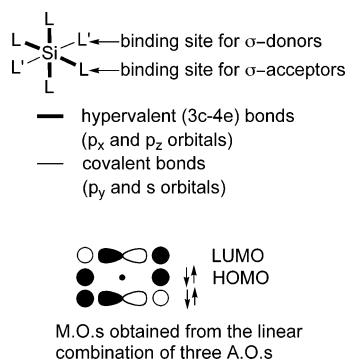

FIGURE 5. Orbital analysis of hypervalent octahedral silicon complexes derived using valence bond theory.

energy donor electron pairs and are considered the more electron-withdrawing positions.

In a complex formed between a bis *N*-oxide, an ionized trichlorosilyl ketene acetal, and a ketone, the "ligands" around the central silicon atom are an enolate oxygen, two chlorine atoms, two *N*-oxides, and a carbonyl oxygen. The chlorine atoms, being the most electronegative elements, would be expected to take on a trans disposition allowing both to comprise a hypervalent 3-center-4-electron bond. The ketene acetal and the ketone would therefore be forced to reside trans to *N*-oxide oxygens. In the absence of orbital degeneracy the ketone can occupy an electron withdrawing sp-hybridized orbital and be activated to nucleophilic attack. Meanwhile, the ketene acetal can bind through an electron-rich hypervalent orbital, trans to a strongly donating *N*-oxide, which would place a larger degree of electron density on the ketene oxygen, thereby increasing the nucleophilicity of the enolate unit. This construct is termed the equato-

rial−equatorial isomer (**vi**, Figure 4). Alternatively, the ketene acetal could also bind in the axial position in a hypervalent orbital (**vii/viii**, Figure 4). In this complex, the ketene acetal would remain nucleophilic due to its bonding through a hypervalent orbital, but it would not be as strongly activated because some electron density would be removed by the trans chlorine atom. Binding of the ketone into an axial position (**ix/x**, Figure 4), trans to a chlorine atom, should be unfavorable as the chlorine atom would prefer this orbital to contain a maximum proportion of p-character (i.e., to be hypervalent), which would formally place a high degree of electron density onto the carbonyl oxygen. Indeed, an extensive computational search failed to find a ground-state structure for complexation of the ketone to this position; the ketone would not remain bound in the coordination sphere of the silicon atom. Thus, complexes **ix** and **x** with axially oriented ketones were ruled out as viable intermediates in the reaction, and only the remaining three complexes **vi**, **vii**, and **viii** were further analyzed.

Each of these complexes is capable of generating either the *S* or the *R* aldolate by exposure of either the *Si*- or *Re*-face of the ketone to the nucleophile in the aldolization process. The six possible transition-state structures (three generating the *S* enantiomer, three generating the *R* enantiomer) were analyzed at the PM3 level. All of the transition-state structures obtained in this study were confirmed to be aldol reaction transition states through IRC analysis and all possess one strong negative mode of vibration. All calculations were carried out using the PC version[34] of the GAMESS (US) QC package.[35]

3.3. Acetophenone. Acetophenone was employed during the catalyst optimization and was therefore used in the initial computational studies. The catalyst structure was based on the parameters determined by X-ray crystallographic analysis of (*P*)-(*R,R*)-**19**·SiCl$_4$, except the *n*-butyl group was truncated to a methyl group for computational simplicity.[36] Transition-state structures corresponding to the aldol reaction were found from each of the six limiting complexes. Two of these (derived from **viii**) were found to be significantly higher in energy (ca. 25 KJmol^{-1}) than the other transition-state structures. The four remaining transition states (derived from **vi** and **vii**) had very similar energies, with only minor differences being observed at the PM3 level. It was noted that the formation of the *S* aldol product was slightly preferred for the **vii** isomer by 0.92 kJ mol^{-1}, whereas the *R* aldol product was slightly preferred for the **vi** isomer by 0.37 kJ mol^{-1}. These results gave no clear indication of the origin of enantioselectivity in the aldol reaction.

3.4. Propiophenone. Despite the lack of a clear distinction, the analysis of these transition-state structures provided important insights into the reaction. The similarity of the transition-state energies suggested that the energetic differentiation among the transition-state structures would be very sensitive to steric interactions and second-order bonding effects between the ketone

(34) Granovsky, A. A. www http://classic.chem.msu.su/gran/gamess/index.html.

(35) Schmidt, M. W. et al. *J. Comput. Chem.* **1993**, *14*, 1347−1363.

(36) In fact, this methoxy catalyst had been tested in the aldol reaction and was found to generate the *S* aldol product from acetophenone albeit in 77.5/22.5 er.
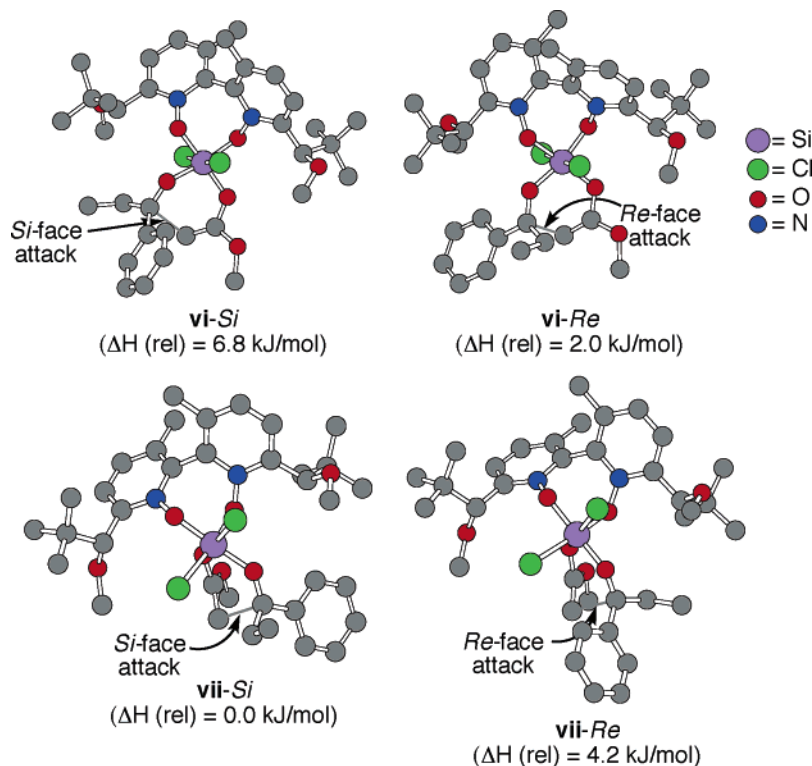
FIGURE 6. Transition-state structures and energies for both the *S* and *R* generating pathways for complexes **vi** and **vii**. Only the energetic differences between the transition states are shown.

acceptor and the remainder of the complex. To test this hypothesis propiophenone (which gave similar results) was analyzed. The atomic density of these transition state structures meant that this small increase in the steric requirement of the ketone might enhance the energetic separation among the diastereomeric transition-state structures.

Here again, both of the transition-state structures obtained from the complexes **viii** were higher in energy than any of the transition states from the other two binding geometries (ca. 26 kJ mol^{-1}).[37] An interesting picture emerged from analysis of the four remaining diastereomeric transition-state structures (Figure 6). Reaction through the complexes **vi** was predicted to be *R* selective, by 4.8 kJ mol^{-1}, and reaction through the complex **vii** was predicted to be *S* selective by 4.2 kJ mol^{-1}. However, the production of the *S*-configured product, through complex **vii**, was favored over the production of the *R* enantiomer from **vi** by 2.0 kJ mol^{-1}, which correctly predicts the stereochemical outcome of the reaction.

A number of important features common to these structures should be mentioned prior to discussion of the differences. First, all the transition state struc-

tures have predominantly flat conformations where the C$-$O$_{ketone}-$Si$-$O$_{ketene}$ torsion angle is approximately 0°. A preference for a more boatlike transition state is favored, especially in the case of the **vii**-*Si* transition-state structure. The long Si$-$O bonds make this assembly energetically acceptable. In all cases, the more chairlike transition-state structures were of higher energy. Second, in all these structures, the methoxy group of the silyl ketene acetal is nearly synplanar with the double bond. Third, the methyl group of propiophenone is always antiperiplanar to the forming bond. Finally, with regard to the catalyst structure, it is interesting that the conformation of the substituents in the 6,6′-position places the methine hydrogen nearly in plane ($\pm$20°) and that the role of the *tert*-butyl group is primarily to direct the alkoxy substituent in toward the substrate-binding pocket.

As part of the search for global saddle points, different binding geometries of the ketone were probed. In the ground state, it is well-known that Lewis acids bind *cis* to the smaller substituent of a ketone.[38] This preference results in the small group (R$_S$) pointing "into" the Lewis acid, whereas the large group (R$_L$) points away from the Lewis acid. However, as can be seen in the structures in Figure 6, this distinction diminishes in the transition states as the carbonyl carbon rotates into bonding contact

(37) The reason for the large energy difference between transition states derived from complexes **vii** and **viii** (i.e., ketone in equatorial positions 1 and 2) is the twisted conformation that the catalyst adopts around the silicon center (see Figure 3A). The 6,6′-substituents are located in the upper right and lower left quadrants of the complex. Because the ketene acetal is bound at an axial position, for aldolization to occur the ketone has to turn down out of the equatorial plane. In position 1, this is acceptable as the bottom right quadrant of the complex is unoccupied (the catalyst occupies the top right). However, in position 2 the R-group of the ketone is forced into the same quadrant of the complex as the 6,6′-subtituent, thereby increasing the energy of this orientation.

(38) (a) Henriksson, U.; Forsén, S. *J. Chem. Soc., Chem. Commun.* **1970**, 1229−1230. (b) Stilbs, P.; Forsén, S. *Tetrahedron Lett.* **1974**, *15*, 3185−3186. (c) Hartman, J. S.; Stilbs, P.; Forsén, S. *Tetrahedron Lett.* **1975**, *16*, 3497−3500. (d) Paris, C.; Torri, G.; Elegant, L.; Azzaro, M. *Bull. Soc. Chim. Fr.* **1974**, 1149−1152. (e) Azzaro, M.; Derrieu, G.; Elegant, L.; Gal, J. F. *J. Org. Chem.* **1975**, *40,* 3155−3157. For a review of Lewis acid−carbonyl complexation see: Ooi, T.; Maruoka, K. In *Modern Carbonyl Reactions*; Otera, J., Ed.; Wiley-VCH: Weinheim, 2000, Chapter 1.
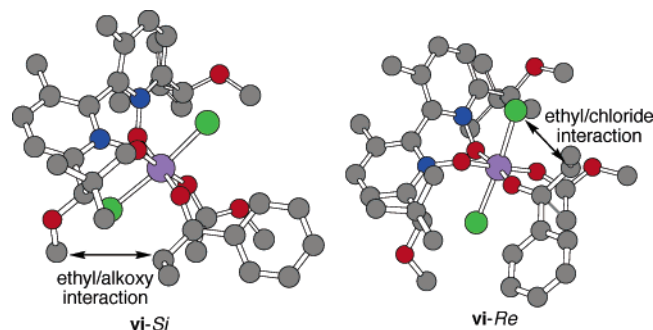
FIGURE 7. Transition state structures for the **vi**-*Si* and **vi**-*Re* pathways. The hydrogen atoms have been removed for clarity.

with the enolate. Nevertheless, the vestige of this preference has an impact on the facial differentiation of the ketone which distinguishes **vi/vii**-*Si* from **vi/vii**-*Re*, in these reactions.

The 4.8 kJ mol^{-1} difference in the transition state structures **vi** arises from steric interactions between the ketone substrate and the 6,6′-substituents on the catalyst. Because the plane of the bound ketone lies approximately perpendicular to the equatorial plane, one of the substituents on the ketone is forced into the space occupied by the alkoxy side chain of the catalyst. In **vi**, the phenyl group points away from the catalyst, thereby placing the ethyl group proximal to the catalyst. The orientations shown in Figure 7 illustrate the decisive interactions between the ethyl group and the 6,6′-substituents in **vi**-*Si* and between the ethyl group and an axial chlorine atom in **vi**-*Si*, thus explaining the *Re* face preference in this complex.

In the complexes **vii**, the situation is reversed because the plane of the bound ketone is now coincident with the equatorial plane. In addition, the carbonyl group is highly distorted in its binding to the silicon such that the Si−O−ketone bond is nearly perpendicular to the carbonyl plane. The decisive interactions as illustrated in Figure 8 are between the ketone groups and the equatorial chlorine atom. In **vii**-*Si*, this interaction is between the ethyl group and the chlorine, whereas in **vii**-*Re* the phenyl group experiences the closest contact. Thus, the *Si*-face attack preference for this complex is based on the difference between an ethyl and a phenyl group. Interestingly, all structures that place the ketone substituents closer to the other equatorial group (*N*-oxide ligand) were much less stable. The implication of this finding is very significant for catalyst design. In this lower energy pathway, variation in the size and nature of the 6,6′-substituents will have little influence on the enantioselectivity. So long as the groups are sufficiently bulky to force the ketone toward the equatorial chlorine, their role is satisfied.[39] Of course, in the complex **vi** the size of these groups does play a role, so the design is complicated by the availability of many pathways of similar energy.

3.5. Catalyst Structure/Selectivity Relationships. The catalyst structure/selectivity relationships in the addition of **1** to acetophenone are supportive of the stereochemical analysis presented above. The alkoxy group at 6,6′-positions was found to influence the enantioselectivity, which increased as the size of the group increased from methyl to mesityl (77.5.22.5 er to 93.5/6.5 er, Table

7). The effect of a change in the size of the ether group would be manifest in an increasing interaction with the ketone which would more seriously destabilize **vi**-*Re* (alkoxy−phenyl interaction) compared to **vi**-*Si* (alkoxy−ethyl interaction). The next result would be a reduction in the reaction flux through pathway **vi**-*Re* resulting in an increase in the *S* enantioselectivity (Figure 7). As mentioned above, the ether group has less of an effect on the pathway via **vii**. The change from an *O*-methyl to an *O*-*n*-butyl group may also be entropic, rather than enthalpic, in origin where rotation of the *n*-butyl chain becomes limited at the transition state.[40] The sharp decrease in rate and enantioselectivity when using the 2,4,6-triisopropylbenzyl derivative (*P*)-(*R,R*)-**22** is likely due to a global destabilization of the entire complex leading to reaction through less favorable pathways.

The effect of changing the size of the substituent at the 6,6′-position illustrates the complexity analyzing multiple pathways of similar energy. The selectivity increased in changing an isopropyl to a *tert*-butyl group but decreased upon further enhancement of steric bulk (Table 2). The reduced selectivity from catalyst (*P*)-(*R,R*)-**25** may be understood in the diminished interaction of this substituent (and the secondary control over the alkoxy orientation). On the other hand, an increase in steric bias at this position has a greater destabilizing effect on the **vii**-*Si* pathway. The ketone substituents point in the quadrant of the complex directly below the substituent on the catalyst (Figure 8). The *tert*-heptyl group projects further down into the quadrant of the complex that the ketone occupies, thus destabilizing the *S* selective pathway. However, in **vi**, it would appear that the **vi**-*Re* pathway would be more affected, thus making firm rationalization difficult.
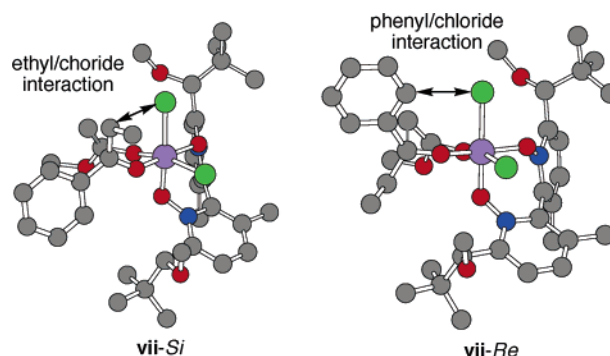

FIGURE 8. Transition-state structures for the **vii**-*Si* and **vii**-*Re* pathways. The hydrogen atoms have been omitted for clarity.

(39) This is of course, the basis for the elimination of reaction pathways via complex **viii** as discussed above.

(40) The magnitude of the entropy change, in rising to the transition state, is likely to be different for each of the diastereomeric transition states. These changes in Δ*S* can be extremely significant as was clearly shown by Ingold in the Finkelstein substitution of organic halides (Ingold, C. K.; De La Mare, P. B. D.; Mackie, J. D. H. *J. Chem. Soc.* **1955**, 3200−3236). The modest improvements in enantioselectivity observed in changing a methyl to an *n*-butyl group represent a very small change in the steric requirement of the catalyst and may be better understood in the decrease in entropy of the alkoxy side chain in the **vi**-*Re* pathway. The major interaction present in the complex **vi**-*Re* is between the ketone and the alkoxy substituent of the catalyst. At the transition state the *n*-butyl chain will be forced into one conformation, freezing out several rotational degrees of freedom.

To increase the stereoselectivity observed in this reaction and to increase the substrate generality is a significant challenge for this catalyst system. Empirical studies have revealed that the enantioselectivity is dominated by the catalyst chiral axis and the stereogenic centers play a secondary role. Extensive variation in the substituents on the pyridine ring and the peripheral position unveiled valuable trends, but selectivities plateaued and were highly substrate dependent. The computational analysis suggests that the problem is not the way in which these catalysts distinguish the *Re* and *Si* pathways, but rather the availability of multiple complexes of kinetic significance. The most obvious direction is to change the enolate to more effectively differentiate the competing pathways through complexes **vi** and **vii**. For example, replacement of one of the chlorine atoms with a methyl or phenyl group would significantly alter the relative energies of the two complexes and the steric interaction with the ketone. Indeed, these enolates are highly reactive in the aldol addition to aldehydes but have not been investigated with ketones.[41]

Conclusions

The first catalytic, enantioselective method for the aldol addition to nonactivated ketone acceptors has been developed. The additions of methyl trichlorosilyl ketene acetal to a wide range of ketones are subject to catalysis by chiral bipyridine bis-*N*-oxide catalysts. The aldol products, β-*tert*-hydroxy esters, have been obtained in excellent yields with most substrates. The enantioselectivity is highly dependent on the structure of the ketone acceptor, with aromatic ketones being the most selective.

Enantiomeric ratios up to 93.5/6.5 have been achieved using chiral bis-*N*-oxide catalyst possessing both central and axial chirality. An X-ray crystal structure of the catalyst bound with silicon tetrachloride ((*P*)-(*R*,*R*)-**19**·SiCl₄) revealed important clues about the binding pocket and the role of various substituents.

On the basis of extensive computational analysis combined with empirical catalyst structure/enantioselectivity relationships, a stereochemical model has been proposed to account for the origin of enantioselection in this aldol process. In this model, the aldol addition proceeds through a manifold of six-membered, boatlike transition structures organized around a cationic silicon center. The energetic differences among the transition states for the aldolization are not large and the origin of the enantiofacial discrimination in each complex is different. The quest for a general solution for the enantioselective aldol addition to ketones continues.

Supporting Information Available: Procedures for the preparation and full characterization of catalysts (*P*)-(*R*,*R*)-**19** and (*M*)-(*R*,*R*)-**19** and complex (*P*)-(*R*,*R*)-**19**·SiCl₄; optimization experiments and aldolization products along with representative procedures for the addition reactions and correlation of absolute configuration of **3a** and **3bc**; complete refs 10b and 35. This material is available free of charge via the Internet at http://pubs.acs.org.

(41) Denmark, S. E.; Winter, S. B. D. *Synlett* **1997**, 1087−1089.

JO0506276